

## Supplementary Materials for

### Origin of alkylphosphonic acids in the interstellar medium

Andrew M. Turner, Matthew J. Abplanalp, Alexandre Bergantini, Robert Frigge, Cheng Zhu, Bing-Jian Sun, Chun-Ta Hsiao, Agnes H. H. Chang\*, Cornelia Meinert\*, Ralf I. Kaiser\*

\*Corresponding author. Email: ralfk@hawaii.edu (R.I.K.); hhchang@gms.ndhu.edu.tw (A.H.H.C.); cornelia.meinert@unice.fr (C.M.)

Published 7 August 2019, *Sci. Adv.* **5**, eaaw4307 (2019)

DOI: 10.1126/sciadv.aaw4307

#### This PDF file includes:

##### Supplementary Text

Table S1. Infrared absorption peaks before and after irradiation for  $\text{PH}_3 + \text{H}_2\text{O}/\text{H}_2^{18}\text{O} + \text{CH}_4/^{13}\text{CH}_4$ .

Table S2. PI-ReTOF-MS ion counts detected from irradiation of the  $\text{PH}_3 + \text{H}_2\text{O} + \text{CH}_4$  ice mixture and confirmed using  $\text{H}_2^{18}\text{O}$  and  $^{13}\text{CH}_4$ .

Table S3. Identified alkylphosphonic acids and phosphorus oxoacids as trimethylsilyl derivatives by GC×GC-TOF-MS.

Table S4. Quantities of identified alkylphosphonic acids and phosphorus oxoacids in the  $\text{PH}_3/\text{H}_2\text{O}/^{13}\text{CH}_4$  ice mixture and the irradiation yield (molecules  $\text{eV}^{-1}$ ).

Fig. S1. Temperature programmed desorption profiles associated with mass-to-charge ratios ( $m/z$ ) of  $\text{H}_5\text{CPO}$ ,  $\text{H}_5\text{CPO}_2$ ,  $\text{H}_5\text{CPO}_3$ , and  $\text{H}_5\text{CPO}_4$ .

Fig. S2. Calculated ionization energies (IE) and relative isomeric energies ( $\Delta E$ ) for the isomers of  $\text{H}_5\text{CPO}$ ,  $\text{H}_5\text{CPO}_2$ ,  $\text{H}_5\text{CPO}_3$ , and  $\text{H}_5\text{CPO}_4$ .

Fig. S3. Organophosphorus compounds detected in the room temperature residues irradiated ices composed of  $\text{PH}_3/\text{H}_2^{18}\text{O}/\text{CH}_4$  by multidimensional gas chromatography.

Fig. S4. Organophosphorus compounds detected in the room temperature residues irradiated ices composed of  $\text{PH}_3/\text{H}_2\text{O}/^{13}\text{CH}_4$  by multidimensional gas chromatography.

Fig. S5. Time-of-flight mass spectra of silylated phosphorus compounds identified in the residue from irradiated ices of  $\text{PH}_3/\text{H}_2\text{O}/^{13}\text{CH}_4$ .

Fig. S6. Time-of-flight mass spectra of silylated phosphorus compounds in the residue from irradiated ices of  $\text{PH}_3/\text{H}_2^{18}\text{O}/\text{CH}_4$ .

Fig. S7. Time-of-flight mass spectra of silylated methylphosphonic acid identified in residues of ices  $\text{PH}_3/\text{H}_2^{18}\text{O}/\text{CH}_4$  and  $\text{PH}_3/\text{H}_2\text{O}/^{13}\text{CH}_4$ .

References (37–43)

## Supplementary Text

**Photoionization Energy Generation.** The experiments were performed at two distinct vacuum ultraviolet (VUV) photoionization energies generated via four-wave mixing: the first at 10.49 eV ( $\omega_{\text{VUV}} = 3\omega_1$ ) using the third harmonic ( $\omega_1$ , 354.6 nm) of a neodymium-doped yttrium aluminum garnet laser (Nd:YAG, Spectra Physics, PRO-250, 30 Hz) and xenon as the non-linear medium. The second photoionization energy at 9.93 eV ( $\omega_{\text{VUV}} = 2\omega_1 - \omega_2$ ) was prepared by combining the output from the Nd:YAG laser's second harmonic ( $\omega_1$ , 532 nm) and from a second Nd:YAG laser, which used 532 nm to pump a Rhodamine 610/640 dye solution to produce 607 nm, which after undergoing a tripling process ( $\omega_2$ , 202 nm) was mixed with  $\omega_1$  using krypton as the non-linear medium. The VUV photons were separated from the other photons using a lithium fluoride biconvex lens (ISP Optics) and passed 1 mm above the ice mixture. The ReTOF-MS analyzed any ionized molecules by correlating the arrival time with mass-to-charge ratios with an amplified signal from a fast preamplifier (Ortec 9305) and 4 ns bin width triggered at 30 Hz (Quantum Composers, 9518).

**GC×GC-TOFMS Analysis.** Sample-handling glassware was wrapped in aluminum foil, and heated at 773 K for 5 h prior to usage. Eppendorf tips were sterile and the water used for extraction, standard solutions, and blanks had been prepared by a Millipore Super-Q water filter system (4 ppb total organic carbon). The derivatization reagent *N,O*-bis(trimethylsilyl) trifluoroacetamide (BSTFA) with 1% trimethylsilyl chloride (TMCS), the internal standard methyl laurate, hexane, as well as phosphorus standards (methylphosphonic acid, ethylphosphonic acid, *n*-propylphosphonic acid, phosphonic acid ( $\text{HPO}(\text{OH})_2$ ), and phosphoric acid ( $\text{H}_3\text{PO}_4$ )) were purchased from Sigma Aldrich. The residues were extracted with  $10 \times 50 \mu\text{L}$  water from their silver wafers and transferred into conical reaction vials (1 mL V-Vial, Wheaton). The aqueous extracts were dried under a gentle stream of nitrogen and silylated with an excess of  $50 \mu\text{L}$  BSTFA / TMCS (99 : 1) for 90 min at 338 K. The mixtures were cooled to room temperature and subsequently dried under a gentle stream of nitrogen. A final volume of  $30 \mu\text{L}$  of the internal standard methyl laurate ( $10^{-5}$  M) in hexane was added to each reaction vial, mixed with a vortex mixer and transferred into GC vials prior their analyses by two-dimensional gas chromatography time-of-flight mass spectrometry (GC×GC-TOFMS). Procedural blanks were run in sequence to each sample in order to monitor significant background interferences.

The multidimensional analysis was carried out by a GC×GC Pegasus IV D instrument coupled to a time-of-flight mass spectrometer (LECO Corp.). The MS system operated at a storage rate of 150 Hz, with a 25–400 amu mass range, a detector voltage of 1.5 kV, and a solvent delay of 12 min. Ion source and injector temperatures were set to 503 K. The column set consisted of a DB-5ms Ultra Inert column (30 m × 0.25 mm, 0.25 μm film thickness) in the first dimension and a DB Wax in the second dimension (1.4 m × 0.1 mm, 0.1 μm film thickness, Agilent J&W). Helium was used as carrier gas at a constant flow of 1 mL min<sup>-1</sup>. All samples and standard compounds were injected with an identical temperature program in the splitless mode. The temperature of the primary column was held at 313 K for 1 min then increased to 488 K at a rate of 5 K min<sup>-1</sup> followed by an isothermal hold for 4 min. The secondary oven used a temperature off-set of 288 K. A modulation period of 4 s was applied. All standard compounds used to produce calibration curves were injected 3 times and each ice sample 6 times in order to accurately calculate peak areas with reliable statistical error bars. Data were processed using the LECO Corp. Chroma TOFTM software. Compound identification was performed by comparison with the chromatographic retention in both dimensions and mass spectra of authentic standards (Tables S3 & S4, Figures S3–S7).

**Results. PI-ReTOF-MS.** The detection of subliming molecules via photoionization reflectron time-of-flight mass spectrometry (PI-ReTOF-MS) with molecular formulas consistent with methyl phosphorus oxoacids include H<sub>5</sub>CPO (m/z = 64), H<sub>5</sub>CPO<sub>2</sub> (m/z = 80), H<sub>5</sub>CPO<sub>3</sub> (m/z = 96), and H<sub>5</sub>CPO<sub>4</sub> (m/z = 112) (Figure S1). Isomers can be determined by tuning the photon energy to exclude specific isomers as described above in *Experimental*. The results for H<sub>5</sub>CPO<sub>4</sub>, H<sub>5</sub>CPO<sub>2</sub>, and H<sub>5</sub>CPO are presented below, while the main manuscript discusses the results of H<sub>5</sub>CPO<sub>3</sub> with the methylphosphonic acid isomer being the main topic of the preset investigation. *H<sub>5</sub>CPO<sub>4</sub>*. H<sub>5</sub>CPO<sub>4</sub> has two structural isomers (m/z = 112, 113 (<sup>13</sup>C), 120 (<sup>18</sup>O)): methylphosphate (CH<sub>3</sub>OP(O)(OH)<sub>2</sub>) (**XVII**) and hydroxymethylphosphonic acid (HOCH<sub>2</sub>P(O)(OH)<sub>2</sub>) (**XVI**). Signal at m/z = 112 (PH<sub>3</sub>/H<sub>2</sub>O/CH<sub>4</sub>) and 113 (PH<sub>3</sub>/H<sub>2</sub>O/<sup>13</sup>CH<sub>4</sub>) can also contribute from H<sub>7</sub>CP<sub>3</sub> isomers like methyltriphosphane (CH<sub>3</sub>P<sub>3</sub>H<sub>4</sub>), whereas ion counts at m/z = 120 (PH<sub>3</sub>/H<sub>2</sub><sup>18</sup>O/CH<sub>4</sub>) originate from H<sub>5</sub>CP<sup>18</sup>O<sub>4</sub>. However, the lack of any ion counts at m/z = 120 at photon energies of 10.49 eV, which is above the adiabatic ionization energy of both H<sub>5</sub>CPO<sub>4</sub> isomers, leads to the

conclusion that the  $H_5CPO_4$  isomers are either not formed or that their vapor pressure is too low to be detected in the gas phase.

$H_5CPO_2$ . The molecular formula  $H_5CPO_2$  ( $m/z = 80, 81$  ( $^{13}C$ ),  $84$  ( $^{18}O$ )) may account for six isomers. Three isomers have ionization energies above 9.93 eV: methoxyphosphine oxide ( $CH_3OPH_2O$ ) (**X**), hydroxymethylphosphine oxide ( $HOCH_2PH_2O$ ) (**VIII**), and methylphosphinic acid ( $CH_3PH(O)OH$ ) (**IX**). The remaining three isomers hold ionization energies below 9.93 eV: methoxy-hydroxyphosphine ( $CH_3OPHOH$ ) (**VI**), hydroxymethyl-hydroxyphosphine ( $HOCH_2PHOH$ ) (**VII**), and methyl-hypophosphorous acid ( $CH_3PH(OH)_2$ ) (**V**) (Figure S2). The TPD profiles show three sublimation events peaking at about 160 K and 250 K and showing a shoulder at about 300 K. Note that signal at  $m/z = 80$  could also originate from  $H_6CP_2$  isomers such as methyldiphosphine ( $CH_3P_2H_3$ ). This should be mirrored in signal at  $m/z = 81$  in the  $PH_3/H_2O/^{13}CH_4$  system ( $^{13}CH_3P_2H_3$ ). Indeed, a comparison of the TPD profiles and of the early sublimation event peaking at 160 K in particular of  $m/z = 80$  and  $n/z = 81$  suggests the presence of methyldiphosphine ( $CH_3P_2H_3$ ) and  $^{13}C$ -methyldiphosphine ( $^{13}CH_3P_2H_3$ ), respectively, which is absent in the  $PH_3/H_2^{18}O/CH_4$  system at  $m/z = 84$ . Considering the late sublimation event at 250 K, which can be detected in all systems even when lowering the photon energy to 9.93 eV indicates that at least one isomer with an ionization energy less than 9.93 eV is formed (**V**, **VI**, and/or **VII**). Likewise, the shoulder at 300 K disappears in the  $PH_3/H_2^{18}O/CH_4$  system when lowering the photon energy to 10.35 eV. Therefore, a second isomer must have an ionization energy between 10.49 eV and 10.35 eV, i.e. methoxyphosphine oxide ( $CH_3OPH_2O$ ) (**X**).

$H_5CPO$ . The simplest of the one-carbon phosphorus oxoacids,  $H_5CPO$  ( $m/z = 64, 65$  ( $^{13}C$ ),  $66$  ( $^{18}O$ )) can have four isomers: methylhydroxyphosphine ( $CH_3PHOH$ ) (**I**), methoxyphosphine ( $CH_3OPH_2$ ) (**II**), hydroxymethylphosphine phosphine ( $HOCH_2PH_2$ ) (**III**), and methylphosphine oxide ( $CH_3PH_2O$ ) (**IV**). Three notable sublimation events are seen at 10.49 eV at  $m/z = 64$  with peaks at 170 K, 240 K, and 270 K (Figure S1), although the 170 K peak is obscured in the  $PH_3/H_2^{18}O/CH_4$  system by the intense signal at  $m/z = 66$  for diphosphine ( $P_2H_4$ ). The sublimation events at 170 K ( $PH_3/H_2O/CH_4$  and  $PH_3/H_2O/^{13}CH_4$  systems) and 270 K remain at 9.93 eV ionization energy, while the 240 K event vanishes. This confirms the formation and sublimation of methylphosphine oxide ( $CH_3PH_2O$ , IE = 10.20) (**IV**) via the sublimation event at

240 K and the possibility of at least two of the other three isomers that all have ionization energies less than 9.93 eV (**I**, **II**, **III**).

**Results. Infrared & Conversion Yields.** The reactant ratio of the ice was determined using the vibrational modes and absorption coefficients ( $A$ ) for phosphine ( $\nu_2$ , 983  $\text{cm}^{-1}$ ,  $A = 5.1 \times 10^{-17}$   $\text{cm molecules}^{-1}$  and  $\nu_4$ , 1103  $\text{cm}^{-1}$ ,  $A = 7.1 \times 10^{-17}$   $\text{cm molecules}^{-1}$ ), methane ( $\nu_3$ , 3006  $\text{cm}^{-1}$ ,  $A = 6.6 \times 10^{-18}$   $\text{cm molecules}^{-1}$  and  $\nu_4$ , 1300  $\text{cm}^{-1}$ ,  $A = 1.3 \times 10^{-18}$   $\text{cm molecules}^{-1}$ ), and water ( $\nu_L$ , 765  $\text{cm}^{-1}$ ,  $A = 2.7 \times 10^{-17}$   $\text{cm molecules}^{-1}$  and  $\nu_2$ , 1642  $\text{cm}^{-1}$ ,  $A = 9.8 \times 10^{-17}$   $\text{cm molecules}^{-1}$ ). (7, 29) For this determination, the refractive index and density of phosphine ( $n = 1.51$ , 0.90  $\text{g cm}^{-3}$ ), (29, 37) methane ( $n = 1.34$ , 0.45  $\text{g cm}^{-3}$ ), (38) and water ( $n = 1.29$ , 0.94  $\text{g cm}^{-3}$ ) (39, 40) were also utilized. After irradiation, only  $33 \pm 4$  % of the phosphine remained, while  $69 \pm 3$  % of methane and  $75 \pm 10$  % of water did not react. Although two-thirds of phosphine reacted, the initial ratios of 1:10:2 ( $\text{PH}_3:\text{H}_2\text{O}:\text{CH}_4$ ) indicate that approximately equal amounts of phosphine and methane were destroyed while four times as much water reacted. Quantitatively,  $180 \pm 40$  nmol ( $1.1 \pm 0.3 \times 10^{17}$  molecules) of phosphine and  $160 \pm 40$  nmol ( $9 \pm 2 \times 10^{16}$  molecules) of methane were consumed while  $650 \pm 150$  nmol ( $4.0 \pm 0.9 \times 10^{17}$  molecules) of water reacted. The 1:1:4 ( $\text{PH}_3:\text{CH}_4:\text{H}_2\text{O}$ ) reaction ratio is similar the stoichiometric ratio of methylphosphate ( $\text{CH}_3\text{OP}(\text{O})(\text{OH})_2$ ) or methylphosphonic acid ( $\text{CH}_3\text{P}(\text{O})(\text{OH})_2$ ) in excess oxygen, and thus assuming the exclusive formation of either of these products, about 170 nmol ( $1 \times 10^{17}$  molecules) could be produced with  $4.3 \pm 1.5 \times 10^{-4}$  molecules  $\text{eV}^{-1}$  efficiency. Compared to this theoretical value, the GC $\times$ GC-TOFMS analysis (Table S4) detected  $2.90 \pm 0.13$  nmol of methylphosphonic acid (1.7 % yield) and  $78 \pm 1$  nmol of phosphoric acid (46 % yield) in the  $\text{PH}_3/\text{H}_2\text{O}/^{13}\text{CH}_4$  system. This is equivalent to  $7.3 \pm 2.5 \times 10^{-7}$  molecules  $\text{eV}^{-1}$  of methylphosphonic acid and  $2.0 \pm 0.7 \times 10^{-5}$  molecules  $\text{eV}^{-1}$  of phosphoric acid. When accounting for the quantities of phosphonic acid (0.53 nmol, 0.3  $\pm$  0.1 % yield), methylphosphate (0.09 nmol, 0.05  $\pm$  0.1 % yield), ethylphosphonic acid (0.09 nmol, 0.05  $\pm$  0.1 % yield), and n-propylphosphonic acid (0.02 nmol, 0.012  $\pm$  0.002 % yield), nearly half of the reacted phosphorus can be accounted for by these compounds in the residue. In terms of irradiation efficiency, phosphonic acid, methylphosphate, ethylphosphonic acid, and n-propylphosphonic acid yielded  $1.4 \pm 0.5 \times 10^{-7}$  molecule  $\text{eV}^{-1}$ ,  $2.3 \pm 0.8 \times 10^{-8}$  molecule  $\text{eV}^{-1}$ ,  $2.3 \pm 1.2 \times 10^{-8}$  molecule  $\text{eV}^{-1}$ , and  $5 \pm 2 \times 10^{-9}$  molecule  $\text{eV}^{-1}$ , respectively. Much of the remaining phosphorus sublimed during

TPD as diphosphine, triphosphane, and methylphosphine. Thus, methylphosphonic acid was found to be the second most abundant product of the residue after phosphoric acid and several times more abundant than non-methylated phosphonic acid.

**Results. GC×GC–TOFMS.** Trimethylsilylated derivatives of phosphonic acid ( $\text{H}_3\text{PO}_3$ ) and of phosphoric acid ( $\text{H}_3\text{PO}_4$ ) were identified with the molecular ion ( $\text{M}^+$ ) at  $m/z = 226$  and  $314$ , respectively, along with the methyl loss pathways at  $m/z = 211$  and  $299$ , respectively in the solvated residues formed from the  $\text{PH}_3/\text{H}_2\text{O}/^{13}\text{CH}_4$  ices. The molecular ion and methyl loss fragment for phosphoric acid ( $\text{H}_3\text{P}^{18}\text{O}_4$ ) were also detected in the  $\text{PH}_3/\text{H}_2^{18}\text{O}/\text{CH}_4$  system at  $m/z = 322$  and  $307$ , respectively. The mass shifts by 8 amu from  $314$  to  $322$  ( $\text{M}^+$ ) and  $299$  to  $307$  ( $\text{M}-15^+$ ) verify the presence of four oxygen atoms. For phosphonic acid ( $\text{H}_3\text{PO}_3$ ), the fully  $^{18}\text{O}$  labelled form ( $\text{H}_3\text{P}^{18}\text{O}_3$ ) could not be observed since phosphonic acid is known to undergo a facile oxygen exchange upon hydrolysis. Instead,  $\text{H}_3\text{P}^{16}\text{O}^{18}\text{O}_2$  could be monitored through its ( $\text{M}-15^+$ ) ion at  $m/z = 215$ . Note that the phosphonic acid ( $\text{H}_3\text{PO}_3$ ) calibration standard revealed that the ( $\text{M}-15$ )<sup>+</sup> signal was more pronounced than the molecular ion ( $\text{M}^+$ ) by a factor of about 30; therefore, the molecular ion peak was difficult to detect.

The signal for methylphosphate ( $^{13}\text{CH}_3\text{OP}(\text{O})(\text{OH})_2$ ) was detected in the solvated  $\text{PH}_3/\text{H}_2\text{O}/^{13}\text{CH}_4$  residues through  $m/z = 257$  and  $242$  for the molecular ion and methyl loss fragment, respectively. For the  $\text{PH}_3/\text{H}_2^{18}\text{O}/\text{CH}_4$  system, only the  $\text{M}-15^+$  signal was detected at  $m/z = 249$  once again due to the lower intensity of the parent ion compared to the fragment. Likewise, in the  $\text{PH}_3/\text{H}_2^{18}\text{O}/\text{CH}_4$  system, signal shifts by 8 amu from  $m/z = 241$  to  $249$  indicating the presence of four oxygen atoms. These mass spectra can be uniquely assigned to methylphosphate, but not to the hydroxymethylphosphonic acid isomer ( $\text{HOCH}_2\text{P}(\text{O})(\text{OH})_2$ ) since methylphosphate acquires two trimethylsilyl groups during derivatization while three trimethylsilyl groups derivatize hydroxymethylphosphonic acid. This detection signifies the formation of a  $\text{P}(+\text{V})-\text{O}-\text{C}$  bond as present in contemporary phosphorus-containing biomolecules.

Regarding the phosphorus oxoacids,  $7.6 \pm 0.1$   $\mu\text{g}$  of phosphoric acid ( $\text{H}_3\text{PO}_4$ ) and  $40 \pm 5$  ng of phosphonic acid ( $\text{H}_3\text{PO}_3$ ) translate into a molar ratio of  $150 \pm 10 : 1$ . A comparison of these data

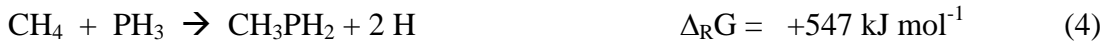
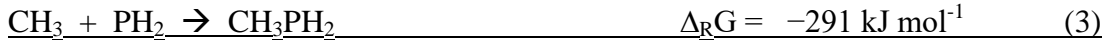
with a detailed infrared spectroscopy analysis (Supplementary Material, Infrared & Conversion Yields) indicates that  $46 \pm 9 \%$  and  $0.3 \pm 0.1 \%$  of the reacted phosphine was converted to phosphoric acid ( $\text{H}_3\text{PO}_4$ ) and phosphonic acid ( $\text{H}_3\text{PO}_3$ ), respectively.

**Results. Comment on Methylphosphate Detection.** Although methylphosphate was not detected in extracts of the Murchison meteorite, Cooper et al. noted that the C–P bond of the alkylphosphonic acids provides substantial stability compared to the phosphate ester bond of methylphosphate, so much so that some phosphonic acids have been shown to persist through heating in hot hydrochloric acid.<sup>(8)</sup> However, acids are known to hydrolyze esters,<sup>(41)</sup> and the use of hydrochloric acid in the sample preparation of the Murchison meteorite may have destroyed any alkyl phosphates originally present in the meteorite. Therefore, our detection of methylphosphate provides evidence that organic phosphates can also be synthesized in interstellar ices alongside organic phosphonates and subsequently incorporated into the early solar system, but these may not have been detected on the Murchison meteorite yet possibly due to the sample preparation.

**Results. Reaction Mechanisms.** Having established the synthesis of methylphosphonic acid via PI-ReTOF-MS and GC×GC–TOFMS, we now consider possible formation mechanisms toward this product. It should be noted that these reactions were carried out in the condensed (ice) phase, but not under single collision conditions in the gas phase. Therefore, it is *not* feasible (neither in our lab nor worldwide) to determine the efficiency of each proposed elementary reaction (oxidation step) involved in the formation of methylphosphonic acid, for instance. This would require pulse-probe experiments with femtosecond (few 10 fs pulses) electron pulses penetrating the ice sample. These experiments do not exist yet. However, based on the molecular structures of the reactants and products ( $\text{CH}_3\text{P}(\text{O})(\text{OH})_2$ ), we identify two potential routes essentially involving the oxidation of methylphosphine ( $\text{CH}_3\text{PH}_2$ ) (route I) or the reaction of methane with phosphonic acid  $\text{HP}(\text{O})(\text{OH})_2$  (route II).

**Reaction Mechanisms – Route I:** Previous studies (6) on the irradiation of phosphine with methane ( $\text{CH}_4$ ) and deuterated methane ( $\text{CD}_4$ ) ice mixtures demonstrated that radical recombination of the phosphino ( $\text{PH}_2$ ) radical with the methyl radical ( $\text{CH}_3$ ) was the dominant

pathway (77%) toward the formation of methylphosphine ( $\text{CH}_3\text{PH}_2$ ) compared to carbene ( $\text{CH}_2$ ) insertion into phosphine (8%) or phosphinidene insertion into methane (15%) in processes methane – phosphine ices.



The net reaction forming methylphosphine and two hydrogen atoms from methane and phosphine requires  $547 \text{ kJ mol}^{-1}$  (5.67 eV), which cannot be achieved thermally at 5 K and thus must be initiated by external sources of energy, such as through non-equilibrium chemistry initiated by the implanted electrons.(25)

Having formed methylphosphine ( $\text{CH}_3\text{PH}_2$ ), oxidation of the phosphorus may convert methylphosphine to methylphosphonic acid ( $\text{CH}_3\text{P}(\text{O})(\text{OH})_2$ ). This formally requires three oxygen atoms. Upon interaction of water ( $\text{H}_2\text{O}$ ) with ionizing radiation, the water molecules can undergo unimolecular decomposition via, for instance, reactions (5) and (6). The simplest way to reach methylphosphonic acid is the stepwise oxidation of methylphosphine by three singlet oxygen atoms as compiled schematically in equation (7).



**Reaction Mechanisms – Route II:** Route II involves the initial oxidation of phosphine to phosphonic acid ( $\text{H}_3\text{PO}_3$ ) via successive addition/insertion of oxygen atoms from the decomposition of water (equation (6)) to phosphine (equation (8)).



Having formed phosphonic acid, methane and phosphonic acid can decompose to produce the methyl (equation (1)) and phosphonyl radical (equation (10)), which can undergo barrierless radical recombination to form methylphosphonic acid (equation (11)).



It must be noted that these are proposed reactions schemes and the actual formation route to methylphosphonic acid may be even a combination of routes I or II. Ideally, the reaction mechanisms would be derived by fitting concentration profiles of reactants, intermediates, and products through a set of coupled differential equations, (42, 43) but these require accurate measurements of the infrared absorption bands for the products and intermediates of the reaction. Considering similar absorptions of the functional groups for a variety of the products, the overlapping absorption bands prevent a determination of accurate temporal concentration profiles.

**Table S1. Infrared absorption peaks before and after irradiation for PH<sub>3</sub> + H<sub>2</sub>O/H<sub>2</sub><sup>18</sup>O + CH<sub>4</sub>/<sup>13</sup>CH<sub>4</sub>.**

Pristine ice, before irradiation (5 K)			
Assignment	Position with <sup>16</sup> O/ <sup>12</sup> C (cm <sup>-1</sup> )	Position with <sup>18</sup> O/ <sup>12</sup> C (cm <sup>-1</sup> )	Position with <sup>16</sup> O/ <sup>13</sup> C (cm <sup>-1</sup> )
H <sub>2</sub> O (ν <sub>1</sub> )	764	731	775
PH <sub>3</sub> (ν <sub>2</sub> )	983	982	982
PH <sub>3</sub> (ν <sub>4</sub> )	1103	1104	1105
CH <sub>4</sub> (ν <sub>4</sub> )	1300	1300	1293
H <sub>2</sub> O (ν <sub>2</sub> )	1644	1647	1648
PH <sub>3</sub> (ν <sub>1</sub> /ν <sub>3</sub> )	2311	2305	2315
CH <sub>4</sub> (ν <sub>3</sub> )	3006	3006	2997
H <sub>2</sub> O (ν <sub>1</sub> /ν <sub>3</sub> )	3224	3198	3231
CH <sub>4</sub> (ν <sub>1</sub> + ν <sub>4</sub> )	4200	4199	4192
CH <sub>4</sub> (ν <sub>3</sub> + ν <sub>4</sub> )	4297	4296	4281
New peaks after irradiation (5 K)			
ν(P–O)	1014	1034	1008
P <sub>2</sub> H <sub>4</sub> (ν <sub>3</sub> )	1067	1072	1070
ν(P=O)	1153	1132	1155
P <sub>2</sub> H <sub>4</sub> (ν <sub>1</sub> )	2275	n.d.	2280

Reference: (7)

**Table S2. PI-ReTOF-MS ion counts detected from irradiation of the PH<sub>3</sub> + H<sub>2</sub>O + CH<sub>4</sub> ice mixture and confirmed using H<sub>2</sub><sup>18</sup>O and <sup>13</sup>CH<sub>4</sub>.**

Molecular Formula	m/z	Molecular Formula	m/z
H <sub>5</sub> CP <sup>+</sup>	48	H <sub>6</sub> CP <sub>2</sub> O <sup>+</sup>	96
H <sub>3</sub> PO <sup>+</sup>	50	H <sub>5</sub> CPO <sub>3</sub> <sup>+</sup>	96
H <sub>6</sub> C <sub>3</sub> O <sup>+</sup>	58	P <sub>3</sub> H <sub>5</sub> <sup>+</sup>	98
H <sub>7</sub> C <sub>2</sub> P <sup>+</sup>	62	H <sub>7</sub> CP <sub>3</sub> <sup>+</sup>	112
H <sub>5</sub> CPO <sup>+</sup>	64	H <sub>4</sub> P <sub>3</sub> O <sup>+</sup>	113
P <sub>2</sub> H <sub>4</sub> <sup>+</sup>	66	H <sub>5</sub> P <sub>3</sub> O <sup>+</sup>	114
H <sub>7</sub> C <sub>2</sub> PO <sup>+</sup>	78	H <sub>5</sub> CP <sub>3</sub> O <sup>+</sup>	128
H <sub>6</sub> CP <sub>2</sub> <sup>+</sup>	80	H <sub>5</sub> P <sub>2</sub> O <sub>4</sub> <sup>+</sup>	131
H <sub>7</sub> C <sub>2</sub> PO <sup>+</sup>	80	H <sub>6</sub> C <sub>2</sub> P <sub>2</sub> O <sub>3</sub> <sup>+</sup>	140
H <sub>5</sub> CPO <sub>2</sub> <sup>+</sup>	80	H <sub>7</sub> CP <sub>2</sub> O <sub>4</sub> <sup>+</sup>	145
H <sub>4</sub> P <sub>2</sub> O <sup>+</sup>	82	H <sub>9</sub> C <sub>2</sub> P <sub>2</sub> O <sub>4</sub> <sup>+</sup>	159
H <sub>9</sub> C <sub>3</sub> PO <sup>+</sup>	92	H <sub>6</sub> P <sub>3</sub> O <sub>4</sub> <sup>+</sup>	163
H <sub>8</sub> C <sub>2</sub> P <sub>2</sub> <sup>+</sup>	94	H <sub>8</sub> CP <sub>3</sub> O <sub>4</sub> <sup>+</sup>	177

**Table S3. Identified alkylphosphonic acids and phosphorus oxoacids as trimethylsilyl derivatives by GC×GC-TOF-MS.**

Compound	$R_{t1}$ [a] [min]	$R_{t2}$ [b] [sec]	$\text{PH}_3/\text{H}_2^{18}\text{O}/\text{CH}_4$		$\text{PH}_3/\text{H}_2\text{O}/^{13}\text{CH}_4$		Standards ( $^{12}\text{C}/^{16}\text{O}$ )	
			$[\text{M}^{++}]$	$[\text{M}-15]^{++}$	$[\text{M}^{++}]$	$[\text{M}-15]^{++}$	$[\text{M}^{++}]$	$[\text{M}-15]^{++}$
Phosphonic acid	13.24	2.92	n.d.	215 <sup>[c]</sup>	226	211	226	211
Methylphosphonic acid	14.20	2.92	246	231	241	226	240	225
Methylphosphate	15.28	3.43	n.d.	249	257	242	256 <sup>[d]</sup>	241 <sup>[d]</sup>
Ethylphosphonic acid	16.12	3.16	n.d.	245	n.d.	241	254	239
n-Propylphosphonic acid	17.52	3.00	n.d.	259	n.d.	256	268	253
Phosphoric acid	17.48	2.68	322	307	314	299	314	299

<sup>[a]</sup>GC×GC retention time 1<sup>st</sup> dimension. <sup>[b]</sup>GC×GC retention time 2<sup>nd</sup> dimension. <sup>[c]</sup>Corresponds to the daughter ion of  $\text{H}_3\text{P}^{16}\text{O}^{18}\text{O}_2$ . <sup>[d]</sup>Standards commercially unavailable.

**Table S4. Quantities of identified alkylphosphonic acids and phosphorus oxoacids in the  $\text{PH}_3/\text{H}_2\text{O}/^{13}\text{CH}_4$  ice mixture and the irradiation yield (molecules  $\text{eV}^{-1}$ ).**

Compound	Molecular Formula	$\text{PH}_3/\text{H}_2\text{O}/^{13}\text{CH}_4$ (nmol) <sup>[a]</sup>	yield molecules $\text{eV}^{-1}$
Phosphonic acid	$\text{HPO}(\text{OH})_2$	$0.53 \pm 0.06$	$1.4 \pm 0.5 \times 10^{-7}$
Methylphosphonic acid	$\text{CH}_3\text{P}(\text{O})(\text{OH})_2$	$2.90 \pm 0.13$	$7.4 \pm 2.5 \times 10^{-7}$
Methylphosphate	$\text{CH}_3\text{OP}(\text{O})(\text{OH})_2$	$0.09 \pm 0.01$	$2.3 \pm 0.8 \times 10^{-8}$
Ethylphosphonic acid	$\text{C}_2\text{H}_5\text{P}(\text{O})(\text{OH})_2$	$0.09 \pm 0.02$	$2.3 \pm 1.2 \times 10^{-8}$
n-Propylphosphonic acid	$\text{C}_3\text{H}_7\text{P}(\text{O})(\text{OH})_2$	$0.02 \pm 0.004$	$5.0 \pm 2.0 \times 10^{-9}$
Phosphoric acid	$\text{H}_3\text{PO}_4$	$78 \pm 1$	$2.0 \pm 0.7 \times 10^{-5}$

The data are mean values from two-dimensional gas chromatographic analyses ( $n = 6$ ) based on  $[\text{M}-15]^{++}$ ; errors shown are 1  $\sigma$  standard deviations.

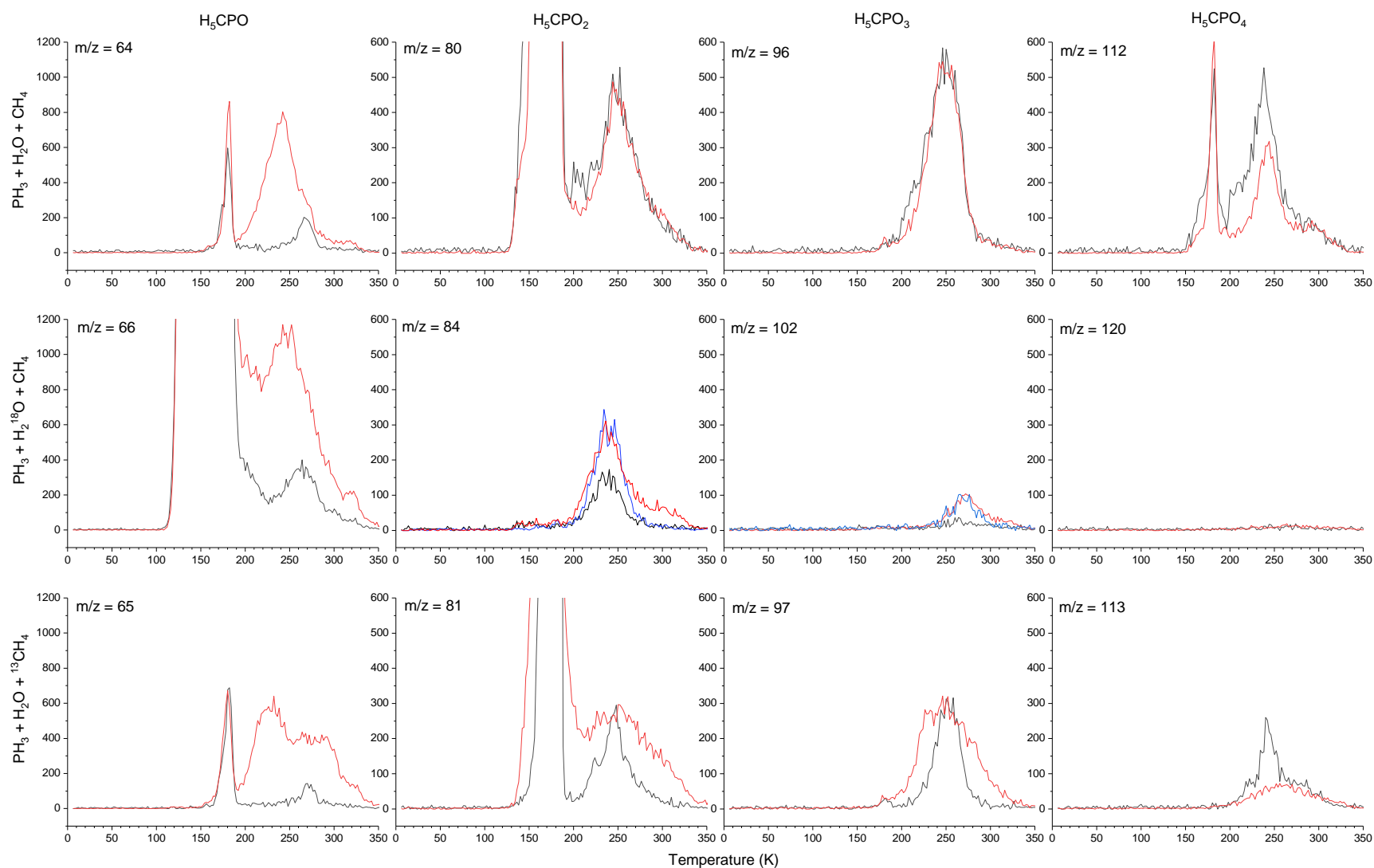


**Fig. S1. Temperature programmed desorption profiles associated with mass-to-charge ratios ( $m/z$ ) of  $\text{H}_5\text{CPO}$ ,  $\text{H}_5\text{CPO}_2$ ,  $\text{H}_5\text{CPO}_3$ , and  $\text{H}_5\text{CPO}_4$ .** Temperature programmed desorption profiles showing ion counts as a function of temperature for  $\text{PH}_3 + \text{H}_2\text{O} + \text{CH}_4$  (top),  $\text{PH}_3 + \text{H}_2^{18}\text{O} + \text{CH}_4$  (center), and  $\text{PH}_3 + \text{H}_2\text{O} + ^{13}\text{CH}_4$  (bottom) associated with the mass-to-charge ratios ( $m/z$ ) of  $\text{H}_5\text{CPO}$  ( $m/z = 64, 66$  ( $^{18}\text{O}$ ),  $65$  ( $^{13}\text{C}$ )),  $\text{H}_5\text{CPO}_2$  ( $m/z = 80, 84$  ( $^{18}\text{O}$ ),  $81$  ( $^{13}\text{C}$ )),  $\text{H}_5\text{CPO}_3$  ( $m/z = 96, 102$  ( $^{18}\text{O}$ ),  $97$  ( $^{13}\text{C}$ )), and  $\text{H}_5\text{CPO}_4$  ( $m/z = 112, 120$  ( $^{18}\text{O}$ ),  $113$  ( $^{13}\text{C}$ )). Temperatures increased to 320 K and were held constant after. The signals are shown for 9.93 eV (black), 10.35 eV (blue), and 10.49 eV (red) photoionization energy.

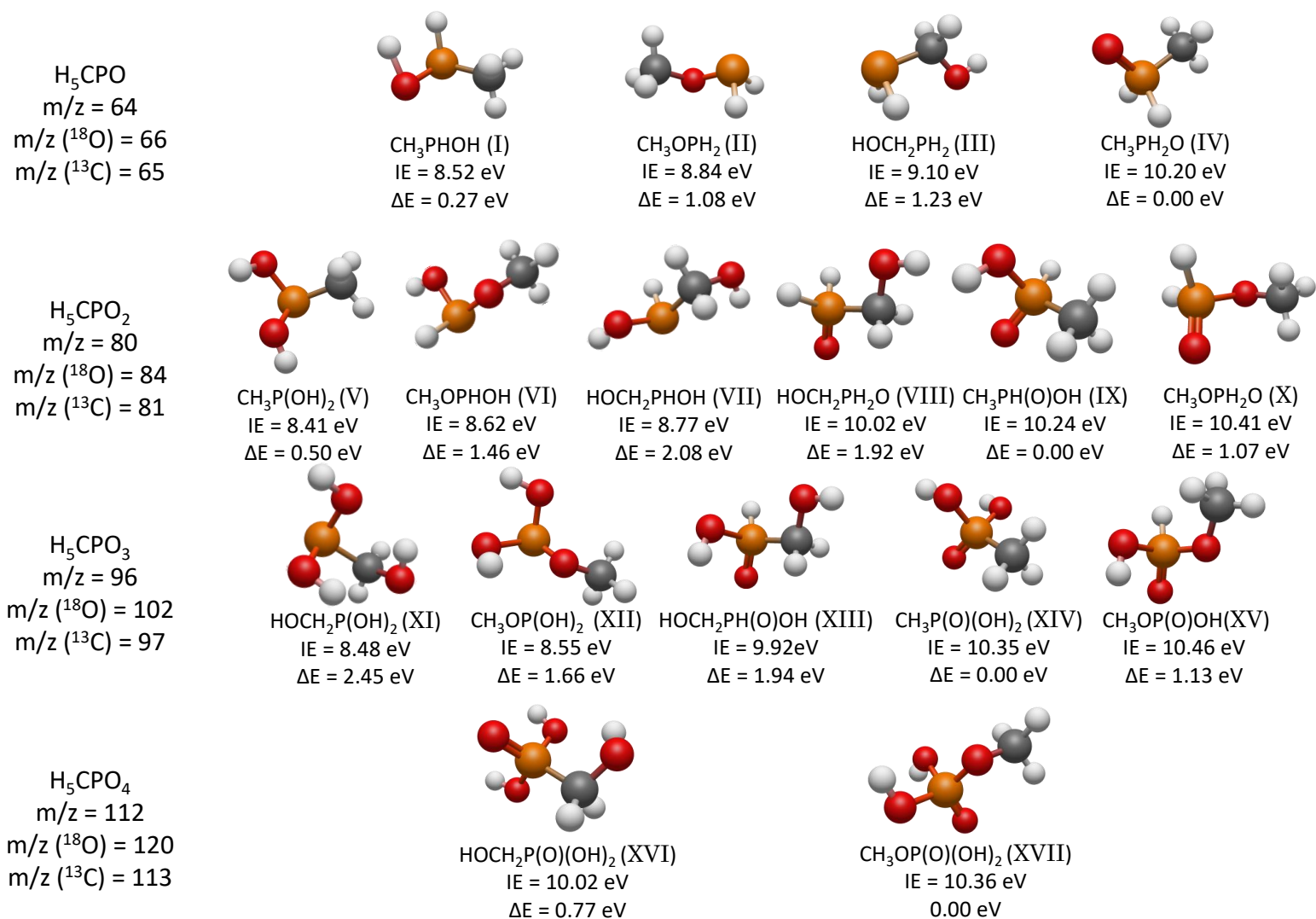
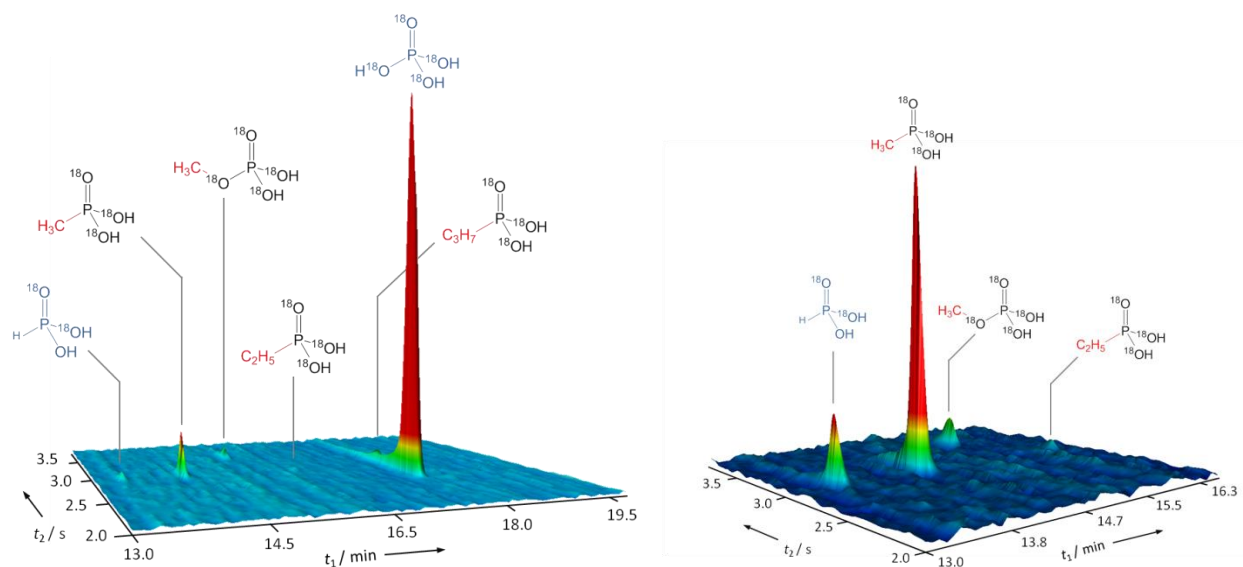
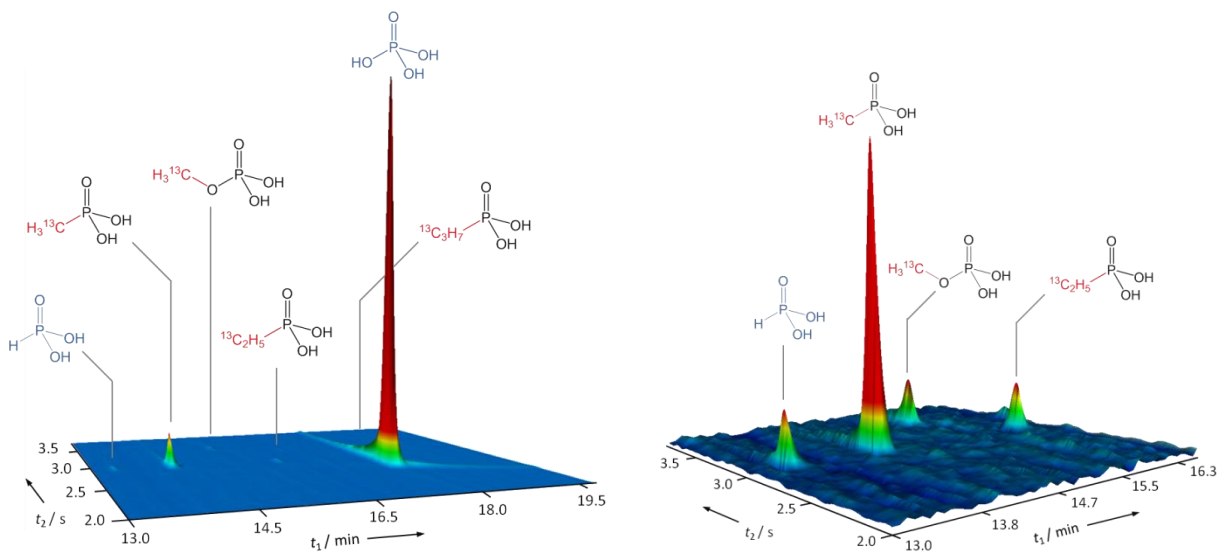


Fig. S2. Calculated ionization energies (IE) and relative isomeric energies ( $\Delta\text{E}$ ) for the isomers of  $\text{H}_5\text{CPO}$ ,  $\text{H}_5\text{CPO}_2$ ,  $\text{H}_5\text{CPO}_3$ , and  $\text{H}_5\text{CPO}_4$ .



**Fig. S3. Organophosphorus compounds detected in the room temperature residues irradiated ices composed of  $\text{PH}_3/\text{H}_2^{18}\text{O}/\text{CH}_4$  by multidimensional gas chromatography.** Atomic mass units  $m/z$  215 ( $\times 20$ ), 231 ( $\times 10$ ), 247 ( $\times 20$ ), 245 ( $\times 20$ ), 259 ( $\times 30$ ), and 307 were selected for the above representation with  $z$ -scaling = 160,000. Right: Partial GC $\times$ GC chromatogram of detected organophosphorus compounds. Atomic mass units  $m/z$  213, 215, 229, 231, 241, 243 ( $\times 10$ ), 245 ( $\times 10$ ) were selected with  $z$ -scaling = 14,000.



**Fig. S4. Organophosphorus compounds detected in the room temperature residues irradiated ices composed of  $\text{PH}_3/\text{H}_2\text{O}/^{13}\text{CH}_4$  by multidimensional gas chromatography.** Atomic mass units  $m/z$  211 $\times 5$ , 226 $\times 5$ , 242 $\times 10$ , 241 $\times 10$ , 256, and 299 were selected for the above representation with  $z$ -scaling = 260,000. Right: Partial GC $\times$ GC chromatogram of detected organophosphorus compounds. Atomic mass units  $m/z$  211 ( $\times 5$ ), 226, 242 ( $\times 10$ ), 241 ( $\times 10$ ) were selected with  $z$ -scaling = 13,000.

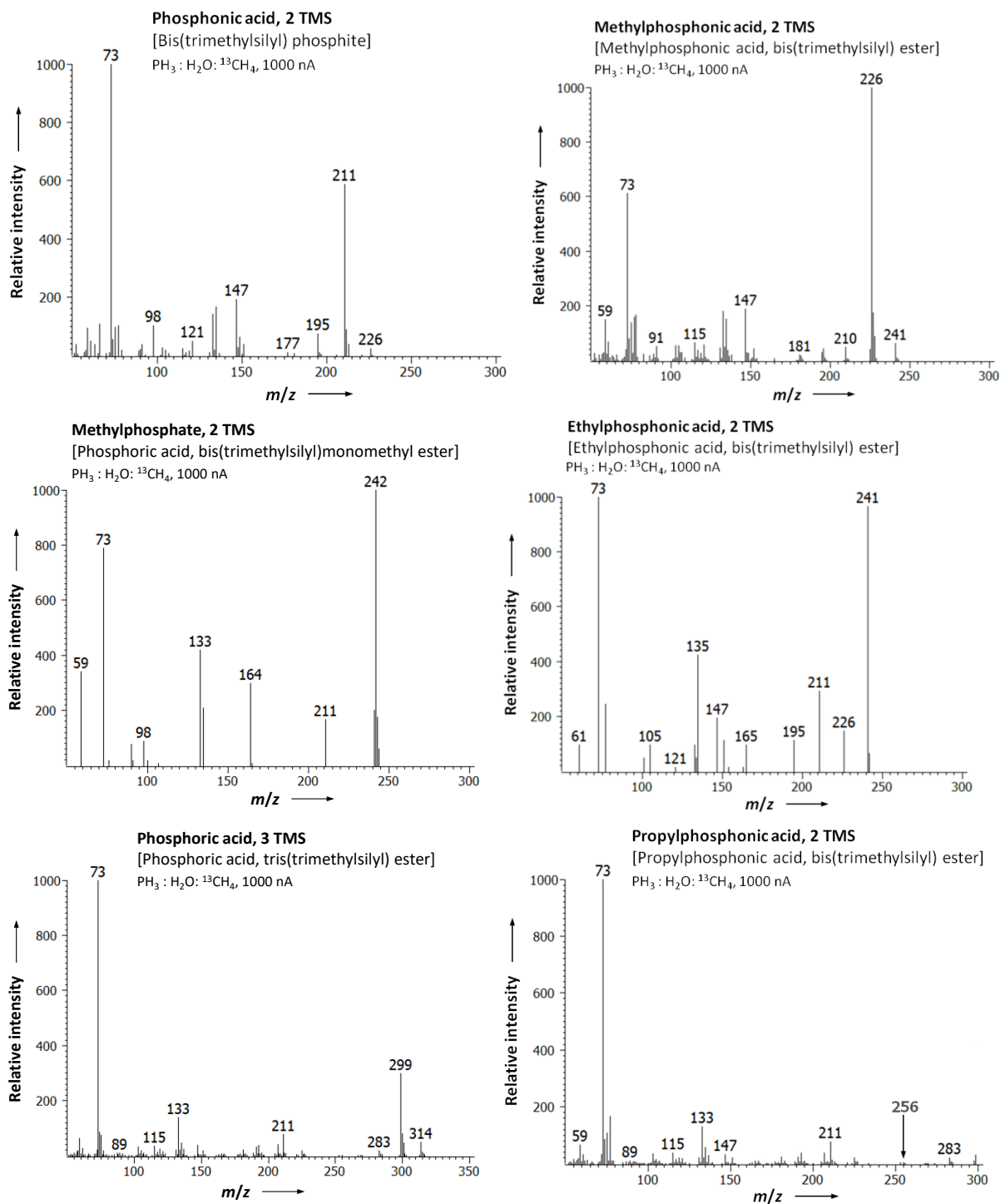


**Fig. S5. Time-of-flight mass spectra of silylated phosphorus compounds identified in the residue from irradiated ices of  $\text{PH}_3/\text{H}_2\text{O}/^{13}\text{CH}_4$ . The  $[\text{M}-15]^{++}$  ion has been used for mass spectral deconvolution.**

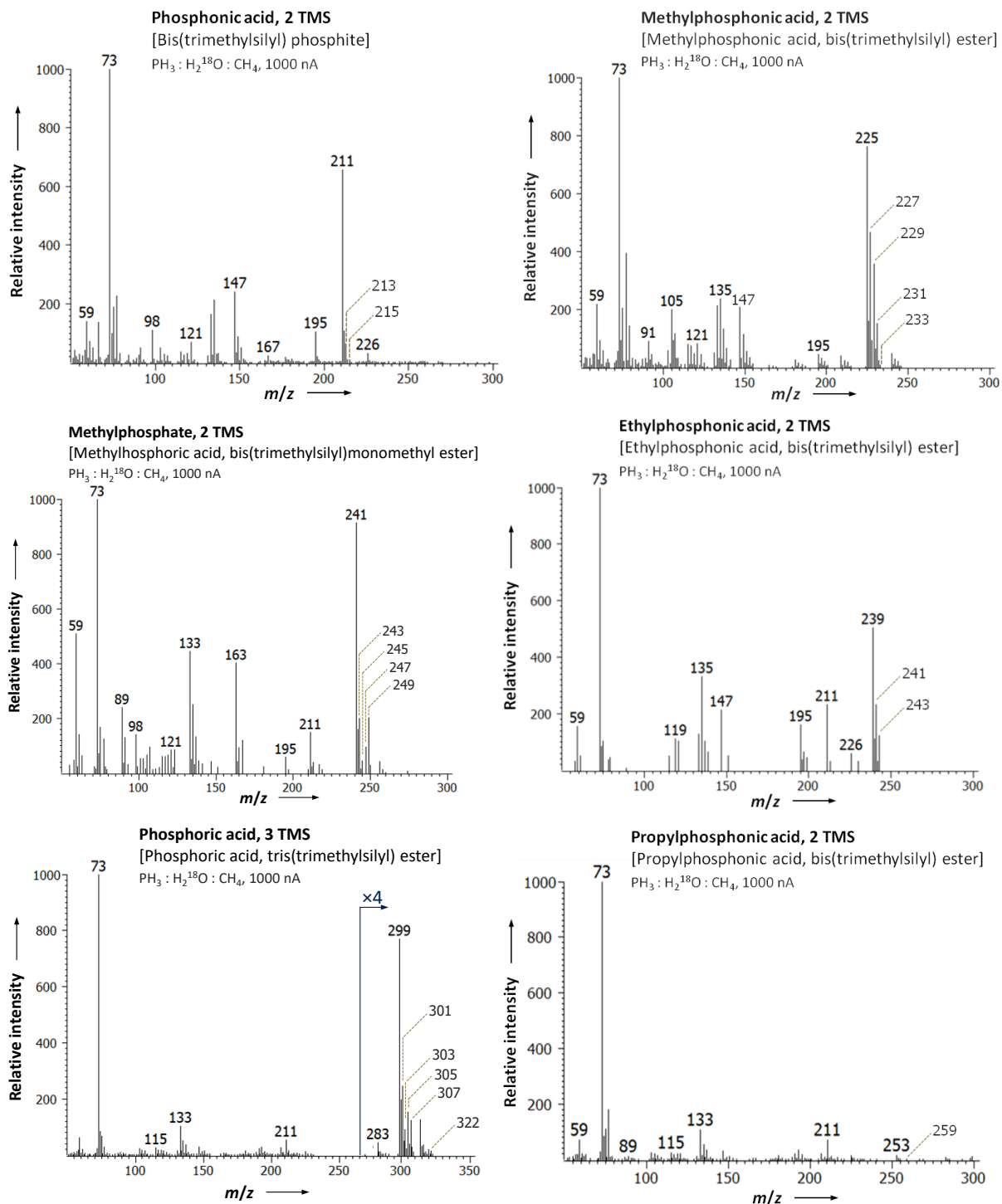


**Fig. S6.** Time-of-flight mass spectra of silylated phosphorus compounds in the residue from irradiated ices of  $\text{PH}_3/\text{H}_2^{18}\text{O}/\text{CH}_4$ . The  $[\text{M}-15]^+$  ion has been used for mass spectral deconvolution.

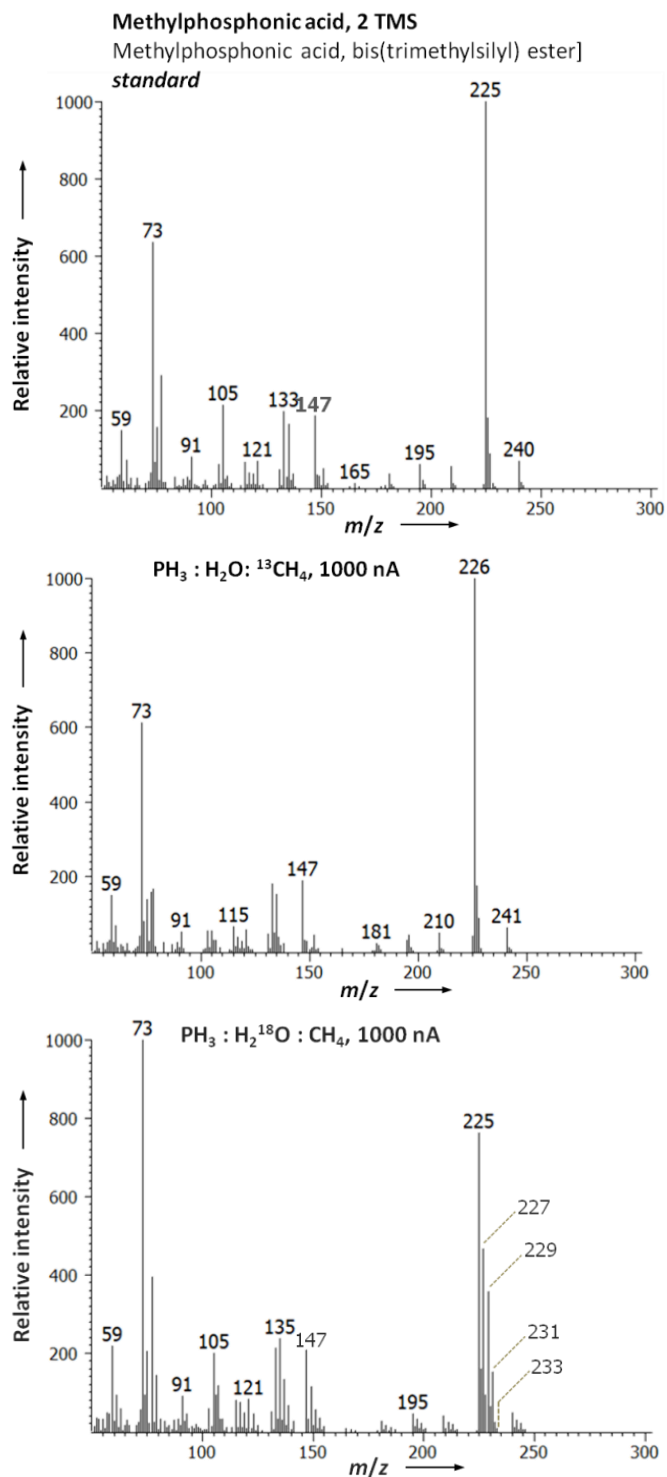


**Fig. S7. Time-of-flight mass spectra of silylated methylphosphonic acid identified in residues of ices  $\text{PH}_3/\text{H}_2^{18}\text{O}/\text{CH}_4$  and  $\text{PH}_3/\text{H}_2\text{O}/^{13}\text{CH}_4$ .** Time-of-flight mass spectra of silylated methylphosphonic acid identified in residues of ices  $\text{PH}_3/\text{H}_2^{18}\text{O}/\text{CH}_4$  (bottom) and  $\text{PH}_3/\text{H}_2\text{O}/^{13}\text{CH}_4$  (center) to the reference standard (top) derivatized and analyzed identically. The  $[\text{M}-15]^+$  ion has been used for mass spectral deconvolution.